Bestätigung der Metadaten/Metadata Approval Sheet

Sehr geehrte Autoren,
Bitte prüfen Sie diese Angaben sorgfältig. Sie sind für alle nachfolgenden Publikationswege (Print, Online, Abstracting und Indexing, Suchmaschinen etc.) relevant. Änderungen sind später nicht mehr möglich. Bitte führen Sie eventuelle Korrekturen in den beschreibbaren Feldern in der rechten Spalte aus. Bitte bestätigen Sie die Korrektheit der Daten, indem Sie das Feld unten anklicken.

Vielen Dank für Ihre Mitarbeit, De Gruyter

Dear author,
Please check these data carefully. They are relevant for all following publication processes in Abstracting and Indexing Services, search engines. They cannot be changed after publication. Please fill in your corrections within the editable fields in the right column. Please confirm the correct data by clicking the field below.

Thanks for your kind cooperation, De Gruyter

Journal-Name: Zeitschrift für Kristallographie
Article-DOI: 10.1515/zkri-2016-1988

Article-Type:

Article-Title: A conformational polymorph of $Ph_3PAu[SC(OEt)=NPh]$ featuring an intramolecular Au···π interaction

Subtitle:

Author 1:
Surname: Yeo
First Name: Chien-Ing
Corresponding: no
E-Mail: no
Affiliation: Research Centre for Crystalline Materials, Sunway University, Faculty of Science and Technology, 47500 Bandar Sunway, Selangor Darul Ehsan, Malaysia

Author 2:
Surname: Loon Tan
First Name: Sang
Corresponding: no
E-Mail: no
Affiliation: Research Centre for Crystalline Materials, Sunway University, Faculty of Science and Technology, 47500 Bandar Sunway, Selangor Darul Ehsan, Malaysia

Chien Ing

Tan

Sang Loon

Author 3:

Surname: Otero-de-la-Roza

First Name: Alberto

Corresponding: yes

E-Mail: alberto@fluor.quimica.uniovi.es

Affiliation: National Research Council of Canada, National Institute for Nanotechnology, 11421 Saskatchewan Drive, Edmonton, Alberta, Canada T6G 2M9

Author 4:

Surname: Tiekink

First Name: Edward R.T.

Corresponding: yes

E-Mail: edwardt@sunway.edu.my

Affiliation: Research Centre for Crystalline Materials, Sunway University, Faculty of Science and Technology, 47500 Bandar Sunway, Selangor Darul Ehsan, Malaysia

History Dates:

Received Date: July 3, 2016

Accepted Date: August 9, 2016

Data checked and receipted ☑ **Date:** August 29th, 2016

Wenn Sie die Korrektheit der Daten nicht durch einen Haken bestätigen oder keine Änderungen in diesem Formular angeben, gehen wir davon aus, dass die angegebenen Daten korrekt sind.

If you don't confirm the correctness by checking the box or implement your corrections in this form, we have to presume that all data are correct.

Q1: Please supply first full name of the author "A. Otero-de-la-Roza" unless this is the name by which the author is commonly known

Chien-Ing Yeo, Sang Loon Tan, A. Otero-de-la-Roza* and Edward R.T. Tiekink*

A conformational polymorph of $Ph_3PAu[SC(OEt)=NPh]$ featuring an intramolecular Au···π interaction

DOI 10.1515/zkri-2016-1988
Received July 3, 2016; accepted August 9, 2016

Abstract: A conformational polymorph, form β, for $Ph_3PAu[SC(OEt)=NPh]$ has been characterised. Like the original structure (form α), the molecule features a linear P–Au–S geometry. The difference between molecular structures rests with the relative disposition of the thiolate ligand which places the N-bound aryl ring in close proximity to the gold centre (form β) rather than the oxygen atom (form α). Density functional theory calculations show the molecule with the Au···π interaction is more stable by 5.2 kcal/mol than the one with the Au···O contact. The molecular packing of both forms are stabilised by C–H···O and C–H···π interactions which make approximately the same contribution to the overall Hirshfeld surfaces. However, key indicators, e.g. crystal packing efficiency and density, and the computational results suggest form β is the thermodynamically favoured form.

Keywords: crystal structure analysis; DFT; gold(I) thiolate; Hirshfeld surface; polymorph; X-ray diffraction.

Introduction

With, R = R″ = Ph and R′ = Et, the title compound, triphenylphosphane-(N-phenyl-O-ethylthiocarbamato-S)-gold(I), (**I**), was one of the first compounds of the general formula $R_3PAu[SC(OR')=NR'']$ to have been structurally characterised [1]. As indicated in Figure 1a, the gold atom lies within a linear geometry defined by phosphane-P and thiolate-S atoms, and the ethoxy-O atom is directed towards the gold centre, forming an intramolecular Au···O contact. This contribution describes a new polymorph of (**I**), whereby there has been a twist about the S–C bond to place the aryl ring in close proximity to the gold centre, as indicated in Figure 1b. The new, conformational [2] polymorph is labelled as form β in order to distinguish it from the original polymorph, form α [1].

The motivation for preparing (**I**) again, leading to the isolation of form β, rests with the exciting biological activity of these compounds. For example, (**I**), along with R′ = Me and iPr, analogues, proved to be highly cytotoxic towards HT-20 colon cancer cell lines [3]. Further, based on a range of mechanistic assays it was determined that apoptosis was induced by both intrinsic and extrinsic pathways. Remarkably, the role of R′ proved crucial in determining cell death with, for example, the compound with the R′ = Me substituent activating the p73 gene and those with R′ = Et (**I**) and iPr activating p53. Such a dependency upon subtle changes in composition permeates biological research in this area. Thus, for the series of compounds R = Ph, R′ = Me, Et and iPr, and R″ = p-tol, the compound with the R′ = Me substituent does not activate either of the p53 or p73 genes, the compound with R′ = Et activates both while the derivative with R′ = iPr upregulates p53 only [4]. Interestingly, this series of compounds also exhibits anti-bacterial activity as they displayed specific bactericidal activity against Gram-positive bacteria, including *Staphylococcus aureus* [5]. The biological motivation for the study of $R_3PAu[SC(OR')=NR'']$ notwithstanding, these and related compounds, e.g. with bidentate phosphane ligands, have proved interesting in terms of crystal engineering endeavours.

The series of compounds $R_3PAu[SC(OMe)-=NC_6H_4NO_2-p]$, for R = Et, Cy and Ph, along with five biphosphane analogues, i.e. containing $Ph_2P–(spacer)–PPh_2$, with spacer = $(CH_2)_n$, for n = 1–4, and ferrocenyl, was the first complete, systematic series of structures obtained in phosphanegold(I) thiolate chemistry pointing to a readiness to crystallise [6]. While the interrelationship between the formation of aurophilic (Au···Au) interactions and solid-state luminescence was the focus of this

***Corresponding authors: A. Otero-de-la-Roza,** National Research Council of Canada, National Institute for Nanotechnology, 11421 Saskatchewan Drive, Edmonton, Alberta, Canada T6G 2M9, E-mail: alberto@fluor.quimica.uniovi.es; and **Edward R.T. Tiekink,** Research Centre for Crystalline Materials, Sunway University, Faculty of Science and Technology, 47500 Bandar Sunway, Selangor Darul Ehsan, Malaysia, E-mail: edwardt@sunway.edu.my
Chien-Ing Yeo and Sang Loon Tan: Research Centre for Crystalline Materials, Sunway University, Faculty of Science and Technology, 47500 Bandar Sunway, Selangor Darul Ehsan, Malaysia

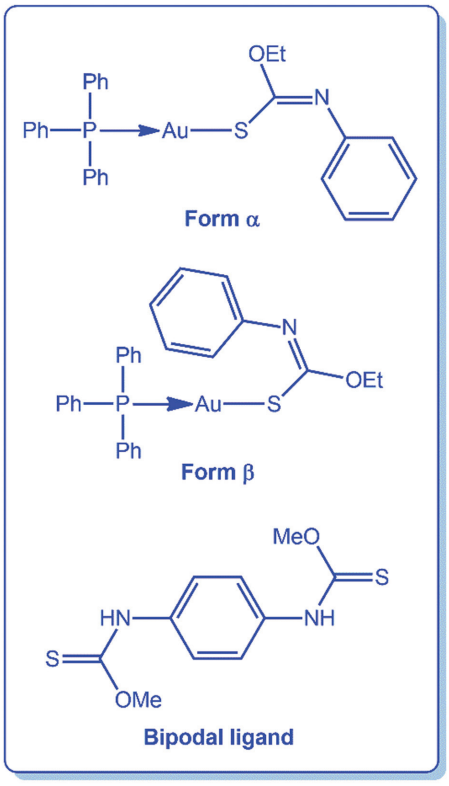

Fig. 1: Chemical diagrams for triphenylphosphane-(N-phenyl-O-ethylthiocarbamato-S)gold(I), (**I**): forms α and β, and of a bipodal thiocarbamide ligand.

study, subsequent studies were undertaken to investigate the relationship of small changes in chemistry upon supramolecular association, e.g. for the series $[(Ph_2P(CH_2)_4PPh_2)\{AuSC(OR')=NC_6H_4Y\text{-}p\}_2]$ for R′ = Me, Et or iPr and Y = H, NO_2 or Me [7]. Particularly relevant to the present study is the series of structures with general formula $R_3PAu[SC(OMe)NR'']$, for R = Ph, o-tol, m-tol or p-tol, and R″ = Ph, o-tol, m-tol, p-tol or $C_6H_4NO_2$-p [8]. By carefully combining the R and R″ substituents it proved possible to induce a rotation about the S–C bond so that the usually observed intramolecular Au···O interaction, e.g. as shown in Figure 1a for **I**, form α, was replaced by an intramolecular Au···π interaction, e.g. Figure 1b; Au···π interactions are now well-documented in supramolecular chemistry involving gold(I) centres as well as gold(III) atoms [9, 10]. A subsequent study of bipodal analogues of monofunctional thiocarbamide molecules, shown in Figure 1c, resulted in the characterisation of three compounds of the general formula $[R_3PAuSC(OMe)=NC_6H_4N=C(OMe)SAuPR_3]$ for R = Et, Cy and Ph [11]. Of interest was that each of the centrosymmetric molecules featured the expected linear coordination geometry but, unexpectedly, intramolecular Au···π interactions. Density-functional theory calculations showed that a Au···π interaction was more stable than a putative Au···O interaction by ca 12 kcal/mol [11].

With the above background in focus, the present contribution describes the crystal and molecular structures of (**I**), form β. The new results are compared with those of (**I**), form α, along with additional structural information provided by DFT methods and Hirshfeld surface analysis.

Experimental

Synthesis and characterisation

The thiocarbamide and triphenylphosphanegold(I) chloride precursors were prepared as described previously [3]. Compound (**I**) was prepared from the stoichiometric reaction of the precursors in the presence of NaOH. Crystals were obtained from the slow evaporation from its dichloromethane/methanol (1/1 v/v) solution held at room temperature, and exhibited the same spectroscopic characteristics as reported earlier [3].

Differential scanning calorimetric (DSC) experiments were carried on a PerkinElmer DSC 8500 (Cooling Device: Intracooler II) at heating rates of 5, 10 and 20 °C/min under a nitrogen atmosphere.

Crystal structure determination

Intensity data for (**I**), form β, were measured at 100 K on a Bruker SMART APEX-II CCD diffractometer with graphite-monochromatised Mo *Kα* radiation (λ = 0.71073 Å). Data processing was achieved with APEX2 and SAINT [12] and the absorption correction was performed with SADABS [13]. Details of unit cell data, X-ray data collection and structure refinement are given in Table 1. The structure was solved by direct methods [14]. Full-matrix least-squares refinement on F^2 with anisotropic displacement parameters for all non-hydrogen atoms was performed with SHELXL-2014/7 [15]. The C-bound H atoms were placed on stereochemical grounds and refined in the riding model approximation with $U_{iso} = 1.2–1.5\ U_{eq}$(carrier atom). Owing to poor agreement, the (5 0 24) reflection was omitted from the final cycles of refinement. The maximum and minimum residual electron density peaks of 0.94 and 1.16 e Å^{-3}, respectively, were located 0.83 and 0.96 Å from the Au atom. A weighting scheme of the form $w = 1/[\sigma^2(F_o^2) + (0.019P)^2 + 2.336P]$ where $P = (F_o^2 + 2F_c^2)/3$ was employed. The programs WinGX [16], ORTEP-3 for Windows [16] QMol [17], PLATON [18] and DIAMOND [19] were also used in the study.

Computational chemistry

Density-functional theory (DFT) calculations, e.g. energy minimisation, were carried out using the Gaussian program [20]. The LC-ωPBE functional [21, 22] combined with the XDM dispersion correction [23, 24] were employed as implemented in the postg program

Tab. 1: Crystallographic data and refinement details for (**1**), form

Formula	$C_{27}H_{25}AuNOPS$
Formula weight	639.48
Crystal colour, habit	Yellow, prism
Crystal size/mm	0.06×0.07×0.12
Crystal system	Monoclinic
Space group	$P2_1/c$
a/Å	9.0057(8)
b/Å	11.1611(10)
c/Å	23.676(2)
β/°	95.5940(10)
V/Å^3	2368.5(4)
Z/Z'	4/1
D_c/g cm^{-3}	1.793
F(000)	1248
μ(Mo $K\alpha$)/mm^{-1}	6.387
Measured data	29364
θ range/°	1.7–27.5
Unique data	5445
R_{int}	0.030
Observed data [$I \geq 2.0\sigma(I)$]	5008
R, obs. data; all data	0.020; 0.047
R_w, obs. data; all data	0.023; 0.047
Largest difference peak and hole (Å^{-3})	0.94, −1.16

[a]Supplementary Material: Crystallographic data (excluding structure factors) for the structures reported in this paper have been deposited with the Cambridge Crystallographic Data Centre as supplementary publication no. CCDC-1445545. Copies of available material can be obtained free of charge, on application to CCDC, 12 Union Road, Cambridge CB2 1EZ, UK, (fax: +44-(0)1223-336033 or e-mail: deposit@ccdc.cam.ac.uk). The list of Fo/Fc-data is available from the corresponding author (ERTT) up to 1 year after the publication has appeared.

[25]. "The bas employed was 6-31+G* t for Au, for which the aug-cc-pV basis set was used plus ctive core potential combination [26].

Hirshfeld surface analysis

The in olecular interactions present in forms α and β of (**I**) were mode y Hirshfeld surface analysis and their corresponding 2D fingerprint plots were generated using Crystal Explorer software (version 3.1) [27]. Briefly, the mapping of normalised contact distance, i.e. d_{norm}, were obtained by computing the sum of inner (d_i) and outer (d_e) distances of any Hirshfeld surface point to the nearest nucleus [28, 29]. A close intermolecular contact with d_{norm} shorter than the sum of relevant van der Waals radii is shown as red in the Hirshfeld surface (negative in value), a contact with d_{norm} close to the sum of van der Waals radii is shown as white (zero in value) while an intermolecular distance longer than the sum of van der Waals radii is shown as blue (positive in value). The d_{norm} surfaces of forms α and β were mapped within the range of −0.14 (red) to 1.61 Å (blue). All hydrogen atom bond lengths were normalised to the standard neutron bond lengths.

Results and discussion

Molecular structure: experimental

During scale-up for further biological studies, see *Introduction*, powder X-ray diffraction (PXRD) patterns were recorded on the bulk material of freshly prepared (**I**), recrystallised from the dichloromethane/methanol (1/1) reaction mixture, and compared with the simulated patterns calculated from single crystal studies (SCXRD) [30]. The measured pattern of the newly synthesised material did not match that calculated from the literature structure of (**I**), reported to be recrystallised from slow evaporations of its chloroform solution [1, 31]. Accordingly, a single crystal structure analysis was conducted revealing a second polymorphic form for (**I**), i.e. form β; the experimental PXRD matched the simulated pattern calculated for form β.

The molecular structure of form β is shown in Figure 2 and selected geometric parameters are given in Table 2. The gold atom is in a linear geometry defined by an S, P donor set with the Au–P bond length shorter than Au–S. Comparing the S1–C1 and C1–N1 bond lengths of the carbonimidothioate ligand with those of the uncoordinated molecule, EtOC(=S)N(H)Ph [32], for which three molecules comprise the asymmetric unit, reveals significant changes consistent with the ligand functioning as a thiolate. There has been a significant elongation of the S1–C1 bond in form β cf. the range of C=S bonds in the free molecule of 1.646(6)–1.652(5) Å, and conversely, there has been reduction in the C1–N1 bond length compared with the free acid where the range of C1–N1 bonds is 1.320(7)–1.327(7) Å. Reflecting the reorganization of π-electron density upon deprotonation and coordination, systematic changes in the bond angles about the N1 and C1 atoms are also noted.

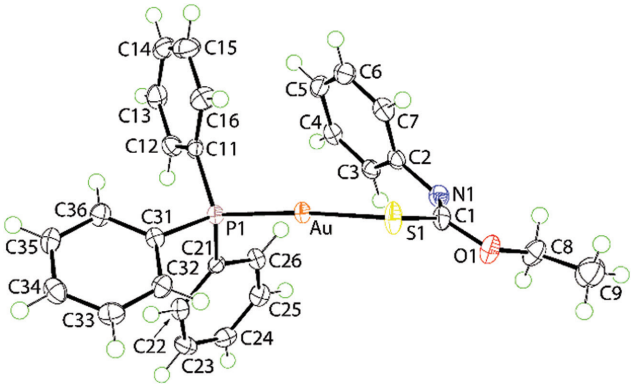

Fig. 2: Molecular structure of $Ph_3PAu[SC(OEt)=NPh]$ (**I**), form β. Displacement ellipsoids are drawn at the 70% probability level.

Tab. 2: Selected geometric parameters (Å, °) for forms α [1] and β of **(I)** and for the energy minimised molecules.

Parameter	Form α [1]	Form β	Calc'd α	Calc'd β
Au–S1	2.303(2)	2.3009(7)	2.31	2.31
Au–P1	2.258(2)	2.2553(7)	2.26	2.27
C1–S1	1.752(8)	1.771(3)	1.76	1.76
C1–O1	1.354(8)	1.359(3)	1.35	1.34
C1–N1	1.262(10)	1.269(4)	1.27	1.27
Au···O1	3.010(6)	–	2.86	–
Au···Cg(C2–C7)	–	3.54	–	3.29
Range of Au···C	–	3.219(3)–4.300(3)	–	3.07–4.02
S1–Au–P1	178.33(8)	175.08(3)	174.6	169.7
Au–S1–C1	103.6(2)	105.57(9)	98.1	107.2
C1–O1–C8	115.1(7)	117.3(2)	117.2	116.9
C1–N1–C8	122.0(7)	123.1(2)	121.1	124.2

The C1–N1–C8 angle in form β has expanded by about 7°, consistent with the formation of the C1=N1 bond. The S1–C1–O1 angle in form β has decreased by ca 16° with concomitant increases in the angles involving the N1 atom, consistent with the single bond nature of C–S and double bond nature of C1=N1.

Geometric data for the original determination of (**I**), form α, are also included in Table 2. The key bond lengths between the two forms are comparable but differences are noted in some bond angles. Notably, the S1–C1–O1 angle has contracted by 6° and that of S1–C1–N1 expanded by 7°, along with an experimentally significant greater distortion of the angle subtended at the gold atom, by 3°. These changes are related to the major conformational difference between the two forms of (**I**), namely a rotation about the C1–S1 bond that places an oxygen (form α) or an aryl ring (form β) in close proximity to the gold atom. It is noted that Au···π(aryl) interactions, occurring both inter- and intra-molecularly in crystal structures have been reviewed previously [9, 10]. The different conformations in the two forms of (**I**) are highlighted in Figure 3, and are discussed further below in *Computational studies*.

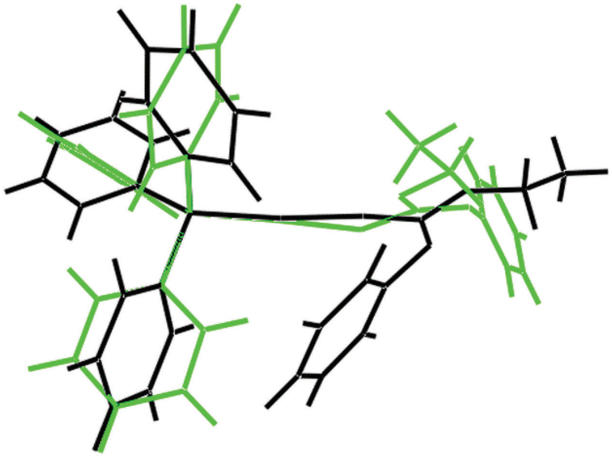

Fig. 3: Overlay diagram of the molecular structures found in the two polymorphs of $Ph_3PAu[SC(OEt)=NPh]$ (**1**). The black molecule corresponds to the structure reported herein, form β, and the other (green) to the original polymorph, form α [1]. The images have been aligned so that the phosphane-bound carbon atoms are overlapped.

Molecular structure: theoretical

In the overwhelming majority of structures related to (**I**), the thiolate ligand is oriented with the oxygen atom close to gold as in form α, rather than the aryl ring, as in form β. The notable exceptions to this were designed by judicious substitution patterns in the N- and P-bound aryl groups in a crystal engineering exercise mentioned in the *Introduction* [8]. Therefore, it was of interest to evaluate the energetics/relative importance of the Au···O/Au···π(aryl) interactions in the conformational polymorphs of (**I**). This was accomplished by employing similar theoretical methods and basis sets reported recently for binuclear gold molecules with related bipodal ligand which also featured intramolecular Au···π(aryl) interactions [11] and for systems having aurophilic interactions [33].

Energy minimization calculations showed that there are two stable conformers each corresponding to an experimental structure and related by a torsion motion around the C–S bond. There is close agreement in the derived geometric parameters of the respective pairs of experimental and calculated molecular structures except for the nature of the weak intramolecular contacts, Table 2. Notably, in both conformations, the intramolecular separation, i.e. Au···O or Au···π(aryl), decreased with a concomitant increased deviation of the P–Au–S

angle from linearity. The observation of the greater distortion of the P–Au–S angle in the structures with the Au···π(aryl) interaction is consistent with the notion that this is more significant than the Au···O interaction [11]. This conclusion is substantiated by further calculations indicating the conformer with the Au···π(aryl) interaction is more stable by 5.2 kcal/mol than the one with the Au···O contact. The calculations reveal the non-dispersion stabilisation is about the same for both the Au···O and Au···π(aryl) contacts, but the dispersion contribution stabilises the Au···π(aryl) interaction relative to Au···O, resulting in the mentioned 5.2 kcal/mol energy difference. Non-covalent interaction (NCI) plots [34] for the two minimum energy structures are shown in Figure 4. The Au···π(aryl) NCI region indicates a stronger and more extensive interaction than Au···O, which manifests as a localised, high density domain. In addition, the NCI plots show that the Au···π(aryl) interaction is further stabilised by π···π interactions between the aryl rings of the thiolate and Ph_3P ligands.

It was thought of interest to also evaluate the energy profile for the rotation around the C–S bond as one conformer was transformed into the other, Figure 5. At rotation angles 0 and 360°, the Au atom and aryl ring are syn, favouring an intramolecular Au···π(aryl) interaction. By contrast, at 180° the Au and O atoms are syn enabling the formation of a Au···O contact. The two conformers are separated by energy barriers between 7 and 8 kcal/mol, confirming the stability of the Au···π(aryl) motif against rotation in the gas phase.

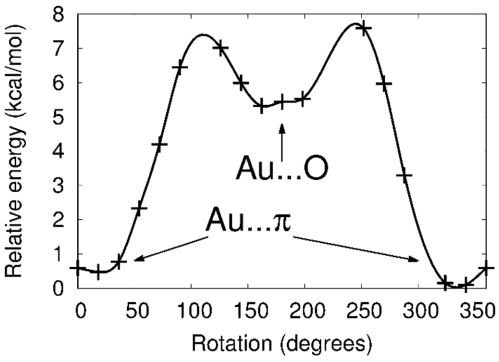

Fig. 5: Energy (kcal/mol) profile as a function of rotation about the C1–S1 bond. At rotation angles = 0 and 360°, the conformation features an intramolecular Au···π(aryl) interaction while that at 180° has an Au···O interaction.

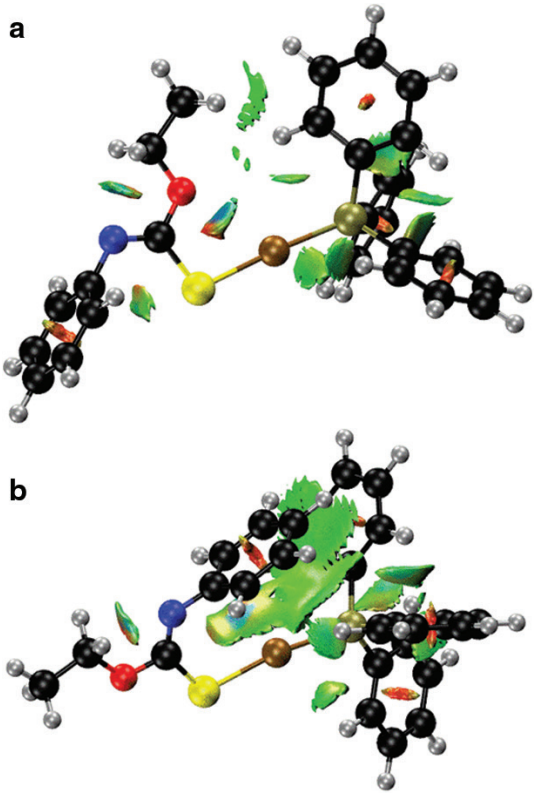

Fig. 4: Non-covalent interaction (NCI) plots for the two conformations observed in $Ph_3PAu[SC(OEt)=NPh]$ (**I**): (a) with an intramolecular Au···O interaction, and (b) an Au···π(aryl) contact.

Molecular packing: experimental

Geometric parameters characterising the intermolecular interactions operating in the crystal structure of form β are collected in Table 3. A three-dimensional architecture featuring both C–H···O and C–H···π interactions is found. Supramolecular layers are formed in the bc-plane, being sustained by P-aryl-C–H···π(N- and P-aryl) interactions, Figure 6a. Connections between layers along the a-axis are of the type C–H···O(ethoxy) as illustrated in Figure 6b.

An overview of the molecular packing of form α is given here as no description was given in the original, brief report of this structure [1]; geometric data are collected in Table 3. As for the β form, both C–H···O and C–H···π interactions are found in the crystal of form α. The former, involving N-aryl-C–H as the donor atom, lead to supramolecular chains with helical topology along the b-axis. These are connected into a three-dimensional arrangement via P-aryl-C–H···π(P-aryl) interactions, Figure 7.

Molecular packing: Hirshfeld surface analysis

In order to gain a deeper understanding of the supramolecular association operating in the molecular packing

Tab. 3: Summary of intermolecular interactions (A–H···B; Å, °) operating in the crystal structures of (**I**): forms α and β.[a]

A	H	B	A–H	H···B	A···B	A–H···B	Symmetry operation
Form β							
C25	H25	Cg(C2–C7)	0.95	2.58	3.444(3)	151	$1-x, -\frac{1}{2}+y, \frac{1}{2}-z$
C35	H35	Cg(C21–C26)	0.95	2.88	3.569(3)	130	$1-x, -y, -z$
C33	H33	O1	0.95	2.59	3.315(3)	133	$-x, 1-y, -z$
Form α							
C6	H6	O1	0.97	2.54	3.502(13)	175	$\frac{1}{2}-x, -\frac{1}{2}+y, -\frac{1}{2}-z$
C34	H34	Cg(C11–C16)	0.97	2.74	3.649(12)	158	$\frac{1}{2}+x, \frac{1}{2}-y, \frac{1}{2}+z$

[a]Cg is the ring centroid of the specified ring.

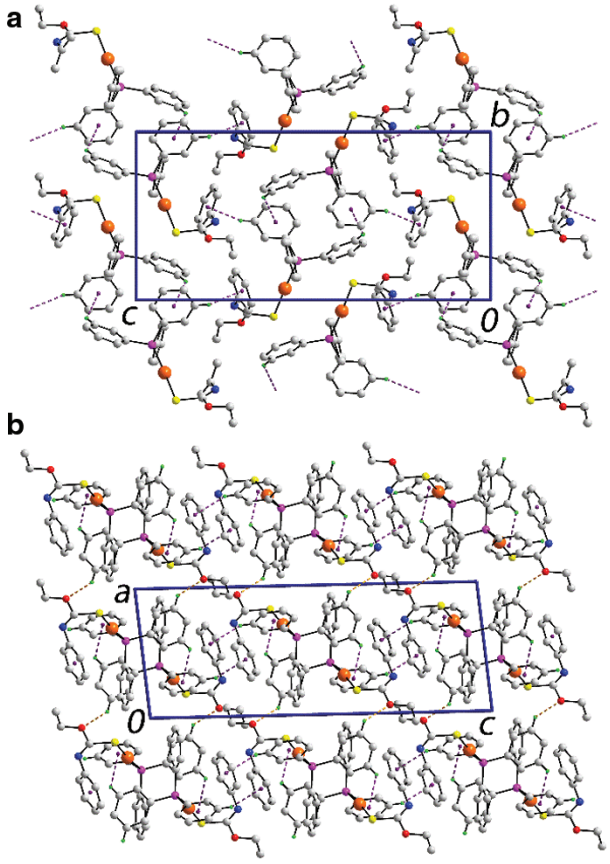

Fig. 6: Two views of the molecular packing in (**1**), form β: (a) supramolecular layer in the bc-plane supported by C–H···π interactions shown as purple dashed lines, and (b) view in projection down the b-axis showing the C–H···O connections between layers as orange dashed lines. Only hydrogen atoms participating in the nominated intermolecular interactions are shown.

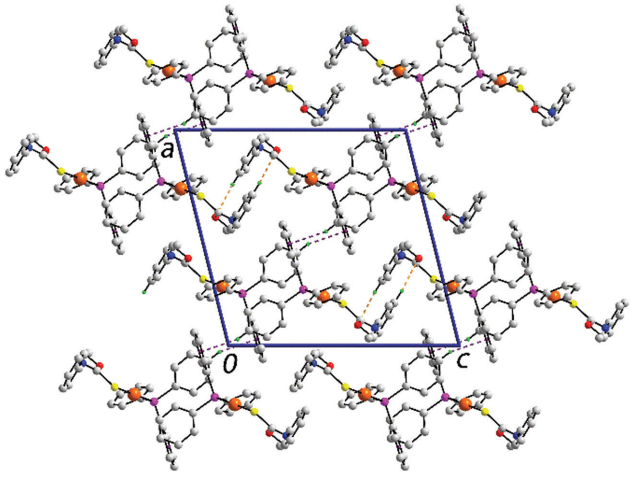

Fig. 7: A view in projection down the b-axis showing the C–H···O and C–H···π interactions as orange and purple dashed lines, respectively. Only hydrogen atoms participating in the nominated intermolecular interactions are shown.

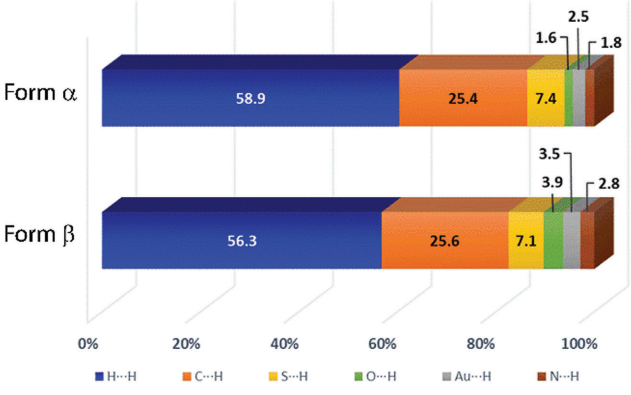

Fig. 8: Percentage contribution of different close contacts to the Hirshfeld surfaces of forms α and β of (**I**).

of polymorphic forms α and β of (**I**), an analysis of their Hirshfeld surfaces was conducted. The percentage contribution of different close contacts to the Hirshfeld surface for forms α and β of (**I**) are plotted in Figure 8. From this, it is clear that there is little difference in the relative contributions to the respective Hirshfeld surfaces, with the dominant contribution being due to H···H contacts, at 58.9 and 56.3% for forms α and β, respectively. The next most significant contribution to t[illegible]urfaces are due to C···H/H···C contacts, at 25.4 and 25.[illegible]espectively. Despite not forming any contacts at distances less than the sum

of the van der Waals radii, S···H/H···S are the next most significant contributors (7.4 and 7.1%, respectively), with all other contacts contributing <5% to the respective Hirshfeld surfaces.

The full two-dimensional fingerprint plots for polymorphic forms α and β are shown in Figure 9a along with views of the d_{norm} surfaces. Even though the most prominent supramolecular synthons operating in the crystals of both forms are of the type C–H···O and C–H···π, the fingerprint plots exhibit distinctive features which arise as a result of the different nature of the C–H···O and C–H···π contacts. The fingerprint plots decomposed into C···H/H···C contacts are shown in Figure 9b. The forceps in form α, with tips at $d_e + d_i \sim 2.7$ Å, contrast the somewhat jagged pincers of form β, with tips at $d_e + d_i \sim 2.6$ Å. Similarly, as seen from Figure 9c, the frog-legs in the fingerprint plot delineated into O···H/H···O contacts with well-defined tips at $d_e + d_i \sim 2.4$ Å for form α contrast the butterfly-wings apparent for form β, with tips $d_e + d_i \sim 2.5$ Å. In short, the analysis of the Hirshfeld surfaces confirm the distinctive packing arrangement in the polymorphic forms of (**I**) but, at the same time, indicates that despite the distinctive conformations found in forms α and β, the relative contributions of the specified intermolecular interactions are comparable.

A comparison between polymorphic forms of (I)

Table 4 presents a summary of some key physiochemical properties for the two forms of (**I**). Immediately evident is that there are some significant differences in the parameters describing forms α and β. The additional "significant" intermolecular interactions in the crystal structure of the β form, Table 3, is consistent with a more compact, globular arrangement, higher density and greater packing efficiency. These parameters suggest that form β is the most stable, thermodynamically favoured form. Regrettably, despite best efforts, it was not possible to isolate

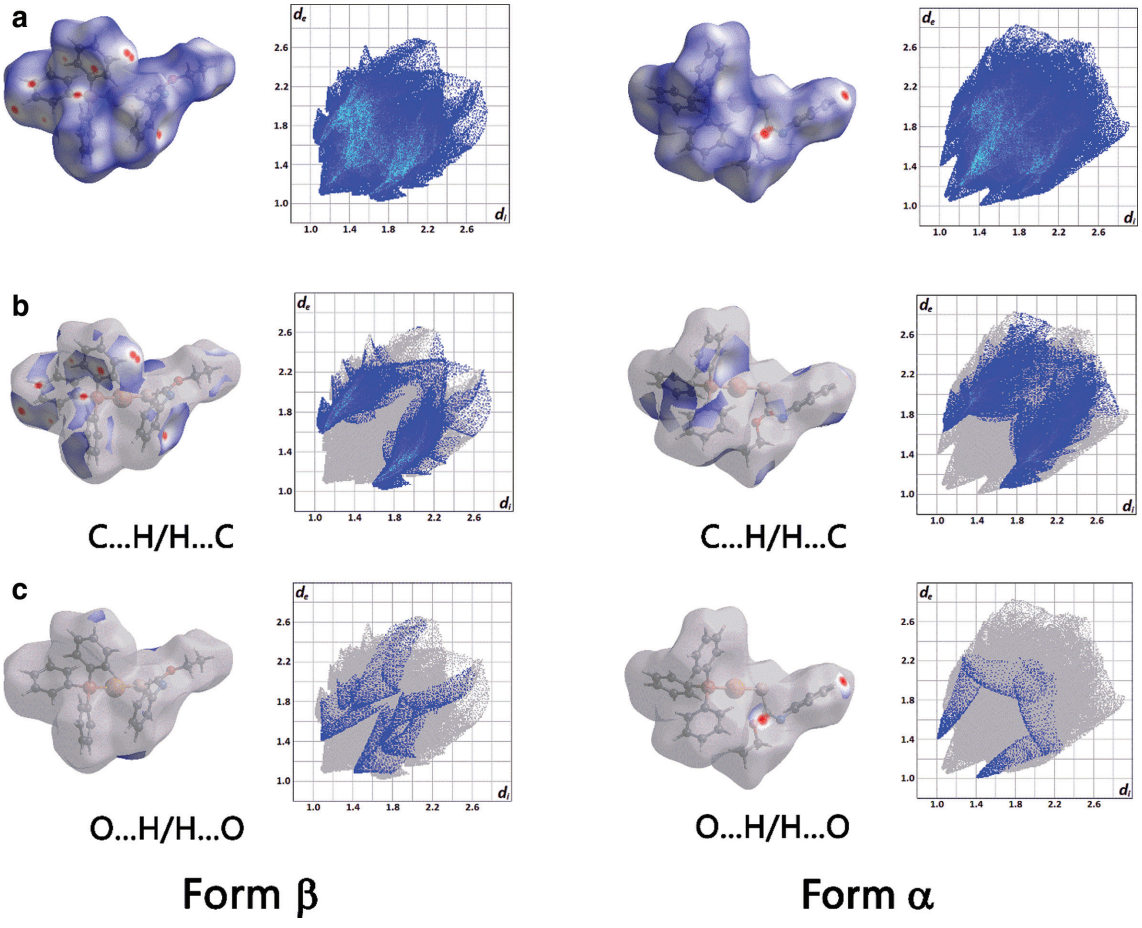

Fig. 9: Comparison between the (a) complete Hirshfeld surface and full fingerprint plots of forms α and β of (**I**), and the corresponding d_{norm} surfaces and two-dimensional plots associated with (b) C···H/H···C and (c) O···H/H···O contacts.

Tab. 4: Physiochemical properties for forms α and II of (**I**).

Property	Form α [1]	Form β
Volume, *V* (Å^3)	630.86	583.22
Surface area, *A* (Å^2)	520.22	466.29
A:*V* (Å^{-1})	0.82	0.80
Globularity, *G*	0.684	0.724
Asphericity, Ω	0.120	0.087
Density (g cm^{-1})	1.657	1.793
Packing index (%)	63.9	69.2

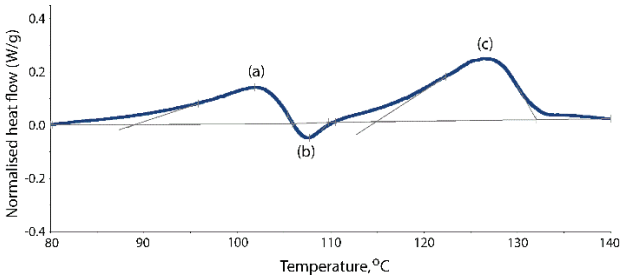

Fig. 10: DSC trace for (**I**), form β measured at 5 °C/min. Step (a): onset = 89.00 °C, end-point = 105.90 °C, peak = 101.86 °C, (b) onset = 106.01 °C, end-set = 109.78 °C, peak = 107.73 °C and (c) onset = 114.89 °C, end-set = 132.05 °C, peak = 126.37 °C.

crystals of form α in order to determine whether definitive interconversion between the polymorphic forms was possible.

DSC measurements were performed on a powdered sample of form β. Three distinct steps were noted with those observed in the scan run at 5 °C/min shown in Figure 10; traces run at 10 and 20 °C/min exhibited similar results. Details of the on-set, end-set and peak temperatures are given in the figure caption. In another experiment, thermogravimetric analysis indicated that decomposition/weight loss of the sample of form β commenced at 170 °C so that any changes in the DSC below this temperature were due to phase changes in (**I**), form β. Recalling that the PXRD indicated the bulk sample comprised form β, the following is offered as a plausible explanation for the three steps observed in the DSC up to 140 °C. Referring to Figure 10, endothermic step (a), ΔH = 11.9 kJ/mol, corresponds to disruption of the crystal structure of form β, exothermic step (b), ΔH = 1.1 kJ/mol, corresponds to crystallisation of a new phase, whereas endothermic step (c) corresponds to melting of the new phase, ΔH = 20.4 kJ/mol. The process was not reversible.

Form α of (**I**) was isolated from its $CHCl_3$ solution and reported to have a melting point of 137–139 °C [1, 31]. Form β, isolated from the methanolic reaction mixture has a melting point of 134–136 °C. Given the elapse of time between the studies, i.e. ca 20 years, different researchers, instruments, etc., these temperature ranges are probably the same. If this assumption is true, a plausible assignment of the DSC events would be disruption of the crystal lattice of form β, crystallisation of form α followed by melting of the latter.

Conclusions

A conformational polymorph, form β, has been characterised for $Ph_3PAu[SC(OEt)=NPh]$ (**I**) which features an intramolecular Au···π interaction rather than the commonly observed Au···O contact as found in form α. Theory suggests the Au···π interaction is more favourable and key physiochemical indicators indicate form β has more efficient crystal packing. Under these circumstances it is likely the conformation featuring the intramolecular Au···π interaction is the thermodynamic outcome from the recrystallisation of (**I**).

Acknowledgments: The staff at Perkin Elmer Malaysia are thanked for measuring the DSC data reported herein. AOR thanks the Spanish Malta/Consolider initiative (no. CSD2007-00045).

References

[1] V. J. Hall, E. R. T. Tiekink, *Z. Kristallogr*. **1993**, *203*, 313.
[2] A. J. Cruz-Cabeza, J. Bernstein, *Chem. Rev*. **2014**, *114*, 2170.
[3] C. I. Yeo, K. K. Ooi, A. M. Akim, K. P. Ang, Z. A. Fairuz, S. N. B. A. Halim, S. W. Ng, H.-L. Seng, E. R. T. Tiekink, *J. Inorg. Biochem*. **2013**, *127*, 24.
[4] K. K. Ooi, C. I. Yeo, K.-P. Ang, A. Md. Akim, Y.-K. Cheah, S. N. A. Halim, H.-L. Seng, E. R. T. Tiekink, *J. Biol. Inorg. Chem*. **2015**, *20*, 855.
[5] C. I. Yeo, J.-H. Sim, C.-H. Khoo, Z.-J. Goh, K. P. Ang, Y.-K. Cheah, Z. A. Fairuz, S. N. B. A. Halim, S. W. Ng, H.-L. Seng, E. R. T. Tiekink, *Gold Bull*. **2013**, *46*, 145.
[6] S. Y. Ho, E. C.-C. Cheng, E. R. T. Tiekink, V. W.-W. Yam, *Inorg. Chem*. **2006**, *45*, 8165.
[7] S. Y. Ho, E. R. T. Tiekink, *CrystEngComm*. **2007**, *9*, 368.
[8] F. S. Kuan, S. Y. Ho, P. P. Tadbuppa, E. R. T. Tiekink, *CrystEngComm*. **2008**, *10*, 548.
[9] E. R. T. Tiekink, J. Zukerman-Schpector, *CrystEngComm*. **2009**, *11*, 1176.
[10] I. Caracelli, J. Zukerman-Schpector, E. R. T. Tiekink, *Gold Bull*. **2013**, *46*, 81.
[11] C. I. Yeo, C.-H. Khoo, W.-C. Chu, B.-J. Chen, P.-L. Chu, J.-H. Sim, Y.-K. Cheah, J. Ahmad, S. N. Abdul Halim, H.-L. Seng, S. Ng, A. Otero-de-la-Roza, E. R. T. Tiekink, *RSC Adv*. **2015**, *5*, 41401.

[12] Bruker. APEX2 and SAINT. Bruker AXS Inc., Madison, Wisconsin, USA, **2009**.
[13] G. M. Sheldrick, SADABS. University of Göttingen, Germany, **1996**.
[14] G. M. Sheldrick, *Acta Crystallogr. A* **2008**, *64*, 112.
[15] G. M. Sheldrick, *Acta Crystallogr. C* **2015**, *71*, 3.
[16] L. J. Farrugia, *J. Appl. Crystallogr.* **2012**, *45*, 849.
[17] J. Gans, D. Shalloway, *J. Mol. Graph. Model.* **2001**, *19*, 557.
[18] A. L. Spek, *J. Appl. Crystallogr.* **2003**, *36*, 7.
[19] K. Brandenburg, DIAMOND. Crystal Impact GbR, Bonn, Germany, **2006**.
[20] M. J. Frisch, G. W. Trucks, H. B. Schlegel, G. E. Scuseria, M. A. Robb, J. R. Cheeseman, G. Scalmani, V. Barone, B. Mennucci, G. A. Petersson, H. Nakatsuji, M. Caricato, X. Li, H. P. Hratchian, A. F. Izmaylov, J. Bloino, G. Zheng, J. L. Sonnenberg, M. Hada, M. Ehara, K. Toyota, R. Fukuda, J. Hasegawa, M. Ishida, T. Nakajima, Y. Honda, O. Kitao, H. Nakai, T. Vreven, J. A. Montgomery, Jr., J. E. Peralta, F. Ogliaro, M. Bearpark, J. J. Heyd, E. Brothers, K. N. Kudin, V. N. Staroverov, R.Kobayashi, J. Normand, K. Raghavachari, A. Rendell, J. C. Burant, S. S. Iyengar, J. Tomasi, M. Cossi, N. Rega, J. M. Millam, M. Klene, J. E. Knox, J. B. Cross, V. Bakken, C. Adamo, J. Jaramillo, R. Gomperts, R. E. Stratmann, O. Yazyev, A. J. Austin, R. Cammi, C. Pomelli, J. W. Ochterski, R. L. Martin, K. Morokuma, V. G. Zakrzewski, G. A. Voth, P. Salvador, J. J. Dannenberg, S. Dapprich, A. D. Daniels, Ö. Farkas, J. B. Foresman, J. V. Ortiz, J. Cioslowski, D. J. Fox, GAUSSIAN 09, Revision A.1, Gaussian, Inc., Wallingford, Connecticut, USA, **2009**.
[21] O. A. Vydrov, G. E. Scuseria, *J. Chem. Phys.* **2006**, *125*, 234109.
[22] O. A. Vydrov, J. Heyd, A. V. Krukau, G. E. Scuseria, *J. Chem. Phys.* **2006**, *125*, 074106.
[23] A. D. Becke, E. R. Johnson, *J. Chem. Phys.* **2007**, *127*, 154108.
[24] A. Otero de la Roza, E. R. Johnson, *J. Chem. Phys.* **2013**, *138*, 204109.
[25] http://gatsby.ucmerced.edu/wiki/Postg.
[26] K. A. Peterson, C. Puzzarini, *Theor. Chem. Acc.* **2005**, *114*, 283.
[27] S. K. Wolff, D. J. Grimwood, J. J., McKinnon, M. J. Turner, D. Jayatilaka, M. A. Spackman, M. A. Crystal Explorer. The University of Western Australia, Western Australia, Australia, **2012**.
[28] M. A. Spackman, D. Jayatilaka, *CrystEngComm.* **2009**, *11*, 19.
[29] J. J. McKinnon, D. Jayatilaka, M. A. Spackman, *Chem. Commun.* **2007**, 3814.
[30] X'Pert HighScore Plus. PANalytical B.V., Almelo, The Netherlands, **2009**.
[31] V. J. Hall, G. Siasios, E. R. T. Tiekink, *Aust. J. Chem.* **1993**, *46*, 561.
[32] R. Taylor, E. R. T. Tiekink, *Z. Kristallogr.* **1994**, *209*, 64.
[33] A. Otero-de-la-Roza, J. D. Mallory, E. R. Johnson, *J. Chem. Phys.* **2014**, *140*, 18A504.
[34] E. R. Johnson, S. Keinan, P. Mori-Sánchez, J. Contreras-García, A. J. Cohen, W. Yang, *J. Am. Chem. Soc.* **2010**, *132*, 6498.

Supplemental Material: The online version of this article (DOI: 10.1515/zkri-2016-1988) offers supplementary material, available to authorized users.

Q2: Please supply accessed date for Ref. [25]

Q3: Please check and confirm the page number and supply volume number for Ref. [29]

Q4: Refs. [31] and [35] were the same in the original manuscript — the duplication was deleted and following references were re-ordered according to numerical order in text and reference list. Please check and confirm

Graphical Synopsis

Chien-Ing Yeo, Sang Loon Tan, A. Otero-de-la-Roza and Edward R.T. Tiekink

A conformational polymorph of $Ph_3PAu[SC(OEt)=NPh]$ featuring an intramolecular Au···π interaction

DOI 10.1515/zkri-2016-1988
Z. Kristallogr. 2016; x: xxx–xxx

Synopsis: A twist about the C–S bond gives rise to conformational polymorphism.